Global Health & Medicine. 2020; 2(5):319-327.
ORIGINAL ARTICLE
DOI: 10.35772/ghm.2020.01092

Early hemodynamics of hepatocellular carcinoma using contrast-enhanced ultrasound with Sonazoid: focus on the pure arterial and early portal phases

Akiko Saito[1,*], Masakazu Yamamoto[2], Satoshi Katagiri[2], Shingo Yamashita[2], Masayuki Nakano[3], Toshio Morizane[4]

[1] Gastroenterology and Hepatology, National Center for Global Health and Medicine, Tokyo, Japan;
[2] Department of Surgery, Institute of Gastroenterology, Tokyo Women's Medical University, Tokyo, Japan;
[3] Tokyo Central Pathology Laboratory Co., LTD, Tokyo, Japan;
[4] Japan Council for Quality Health Care, Tokyo, Japan.

Abstract: To clarify the early hemodynamics of hepatocellular carcinoma (HCC), we defined the early portal phase of contrast-enhanced ultrasound (CEUS) and examined the reliability of this modality for determining HCC differentiation. Starting in 2007, we performed Sonazoid CEUS in 146 pathologically confirmed hepatic nodules; 118 HCC (8 poorly [Pd], 73 moderately [Md] and 37 well-differentiated [Wd]) and 28 benign nodules. We focused on the pure arterial and early portal phases up to 45 seconds after Sonazoid injection, and then the subsequent phase up to 30 minutes. We calculated covariance-adjusted sensitivities for nodule enhancement combinations of these three phases. Nodule enhancements were divided into hypo, iso and hyper. A positive predictive value of 100% was obtained for the following patterns: iso-iso-hypo, hypo-iso-iso, and hypo-hypo-hypo for Wd, hyper-iso-hypo and hyper-hypo-hypo for Md, hypo-hyper-hypo for Pd, and hyper-hyper-hyper for benign nodules. In Wd HCC (early HCC), there were seven enhancement patterns, thought to be characterized by various hemodynamic changes from early to advanced HCC. Two patterns allowing a diagnosis of Wd HCC were hypo in the pure arterial phase. Subsequent iso-enhancement in the early portal phase indicated a portal blood supply. Decreased enhancement in the early portal phase allows a diagnosis of Md HCC. However, gradual enhancement observed from the pure arterial to the early portal phase allows a diagnosis of Pd HCC. Therefore, even in the early portal phase, hemodynamic changes were visible not only in Wd but also in Md and Pd HCC. In conclusion, with division of the early phase hemodynamics into pure arterial and early portal phases, CEUS can provide information useful for determining the likely degree of HCC differentiation and for distinguishing early stage HCC from benign nodules.

***Keywords*:** histological differentiation, early HCC, well-differentiated HCC, contrast-enhanced ultrasonography

Introduction

Contrast-enhanced computed tomography (CT) and magnetic resonance imaging (MRI) are widely used for examining liver tumors. As physicians are primarily responsible for the practical implementation of contrast-enhanced ultrasound (CEUS), the number of patients receiving CEUS is limited. However, due to high sensitivity for identifying target tumors, CEUS is a potentially appropriate imaging modality for detailed evaluation of liver tumors. The 2011American Association for the Study of Liver Diseases (AASLD) guidelines do not recommend CEUS for the diagnosis of hepatocellular carcinoma (HCC) (*1*). The Contrast Enhanced Ultrasound Liver Imaging Reporting and Data System (CEUS LI-RADS) from 2017 does, however, categorize CEUS findings for the differential diagnosis of liver tumors (*2*). In Japan, CEUS plays an important role in the diagnostic algorithm for hepatic tumors (*3*).

As for the ultrasound contrast agent used in Japan, Sonazoid was approved in 2007. The incidence of adverse reactions is low. Unlike SonoVue and Definity, which are used mainly in western countries, Sonazoid is characterized by producing distinct enhancement of the liver parenchyma in the post-vascular phase (Kupffer phase) (*4*). Thus, Sonazoid CEUS is widely used in HCC cases for tumor detection, differential diagnosis, as well as ultrasound-guided treatment navigation and evaluation of treatment responses in post-vascular phase images (*5*). However, few reports have focused on early phase hemodynamics of HCC (*6-8*).

CEUS is superior to other imaging modalities for

visualizing tumor blood flow, though conventional observation is insufficient for detailed evaluation of early phase images characterized by rapid changes in blood flow. Inflow-time mapping has been developed, allowing arterial and portal flows to be displayed separately (*9*). We aimed to investigate the diagnostic ability of CEUS for HCC differentiation using this method. Thus, we observed early hemodynamics on CEUS by dividing the arterial phase into the pure arterial and early portal phases and compared the obtained findings with histopathological features.

Materials and Methods

Patients

Among patients in whom pathologically confirmed hepatocellular nodules (primary HCC and benign nodules, ≤ 5 cm) were obtained during the period from 2007 to 2013 in the Tokyo Women's Medical University, 146 patients with 146 nodules in which Sonazoid-enhanced ultrasound was performed and contrast agent inflow had been identified throughout the tumor, intrahepatic artery, and portal vein in a single section were enrolled in this study. These 146 nodules were comprised of 118 HCC nodules (8 poorly differentiated [Pd], 73 moderately differentiated [Md], and 37 well-differentiated [Wd]) and 28 benign nodules (4 hepatocellular adenoma [HCA], 18 focal nodular hyperplasia [FNH], 3 alcoholic hyperplastic nodules, and 3 large regenerative nodules). All Wd HCC included in this study, except for two nodules obtained by biopsy, corresponded to early HCC (*10*) with stromal invasion (*11*).

Methods

Based on the enhancement differences between the nodules and the surrounding liver parenchyma, nodule enhancements were classified into three levels: hypo-, iso-, and hyper-enhancement. The degree of enhancement was analyzed as one of these three levels, regardless of whether the entire or only part of the nodule showed the enhancement changes.

The imaging phase during CEUS was defined as follows: the pure arterial phase indicated by microbubbles initially appeared in the intrahepatic artery and persisted up to the time immediately before intrahepatic portal flow visualization; the early portal phase was from the first visualization of microbubbles in the portal vein up to 45 seconds after contrast injection; and the subsequent phase was from one minute after injection up to 30 minutes. Based on CEUS patterns obtained from these three imaging phases and four histopathological findings (*i.e.*, Pd, Md, Wd, and benign nodules), Bayes' theorem was applied to calculate the positive predictive value for each of pathological types.

CEUS examination

CEUS was performed by a single ultrasound specialist (with 20 years of experience) within 2 weeks before surgery. Sonazoid was intravenously administered (0.01 mL/kg) through a 21-gauge cannula and flushed with 5 mL of normal saline at a speed of 1 mL/s. We continuously observed tumor enhancement during the initial period of 1-50 seconds, and then again at 1, 2, 3, 5, 10, 20, and 30 minutes (several seconds each). All CEUS images were stored digitally to a hard disk. Two ultrasound specialists (with more than 15 years of experience), both of whom were blinded to the clinical and histopathological findings, reviewed the stored images.

The inflow of microbubbles into the intrahepatic artery (mainly the second branch), followed by that into the portal vein, and increased nodule enhancement as compared with the surrounding liver parenchyma were examined with cine-clip replay. The blood flow distributions within the tumor were observed as required using the inflow-time mapping, in order to assess the arterial and portal blood supplies in the nodules. Inflow-time mapping can demonstrate intensity changes of individual pixels. When saturation intensity reaches 80%, each pixel has a color and an inflow-time map is produced. The blood flow changes during the pure arterial and early portal phases are easily displayed separately by applying different colors representing the inflows into the hepatic artery and portal vein. An additional time-intensity curve was prepared for some nodules to confirm the arterial and portal flows.

The ultrasound device used was a Prosound α-10/F75 with extended Pure harmonic detection, which was operated at a frequency of 1.88 MHz, mechanical index (MI) of 0.18-0.24, dynamic range of 43-50 dB, and frame rate of 15-20 Hz, and Ascendus with wideband pulse inversion mode, which was operated at a frequency of 1.8 MHz, MI of 0.16-0.18, dynamic range of 45-50 dB, and frame rate of 13-20Hz (Hitachi Ltd., Tokyo, Japan).

Histopathological examination

In total, 146 nodules (82 obtained from liver resection and 64 from liver tumor biopsy) of patients enrolled in this study were fixed with formalin and then embedded in paraffin for preparation of 2 or 4 μm sections. The sections were principally stained with hematoxylin-eosin, silver, and Victoria-blue (in some cases, also with CK7 and CD34 stains) for the diagnosis of Wd HCC. Additionally, Hep-Per1, CK-19, and epithelial membrane antigen were stained to differentiate HCC from intrahepatic cholangiocarcinoma. For benign nodules, immunohistochemical staining with specific

tumor markers was performed to make a definitive diagnosis at the pathology department of Teikyo University Hospital (*12*). Two liver pathologists (with more than 20 years of experience) were involved in confirming the diagnosis.

Statistical analysis

The nodule enhancements observed in each of the three different imaging phases were categorized into three levels: hypo, iso, and hyper. In each nodule, each level was given a value of 1 when the nodule was judged to reach the categorized level and 0 otherwise, and then converted into multi-dichotomous values. We calculated crude sensitivities, *i.e*., positive rates, for each category of each imaging phase, simply by calculating the sum of these values divided by the number of nodules as the mean values. The covariance-adjusted sensitivities were calculated, because values which differ between imaging phases are not independent. The covariances for three variables were calculated as the sum of products of the difference between each value, 0 or 1, and the sensitivity, divided by the number of cases (*13*). The covariance-adjusted sensitivity was calculated as $s_1s_2s_3 + s_1cov_{s2s3} + s_2cov_{s1s3} + s_3cov_{s1s2} + cov_{s1s2s3}$, where s stands for the sensitivity, cov stands for the covariance, and the subscript numbers correspond to each of the imaging phases.

In order to calculate the positive predictive value or the posterior probability, we set equal prior probability values, *i.e*., 0.25 for each of the four diagnostic categories: benign nodule, Wd, Md, and Pd HCC. We calculated joint probabilities, the product of sensitivity and prior probability, for each of the three imaging phases and a predictive value as a proportion of each joint probability of the sum of the joint probabilities. We used R (*https://cran.r-project.org/*) for the above calculations with scripts that we devised for our research.

Results

Patient and nodule characteristics

The median age of the enrolled patients was 67 years (33-86 years). There were 107 males and 39 females. The numbers of tumors located in segments 1/2/3/4/5/6/7/8 were 1/11/14/19/22/18/19/42, respectively. The mean tumor sizes were 30 mm (15-50 mm) for Pd, 24 mm (10-50 mm) for Md, 16 mm (10-25 mm) for Wd HCC, and 25 mm (10-50 mm) for benign nodules.

The median times required for microbubbles to reach the intrahepatic artery and the portal vein after injection of Sonazoid were 17 sec (9-27 sec) and 24 sec (14-36 sec), respectively.

Predictive values of enhancement patterns for pathological diagnosis

Analysis of the enhancements of all nodules in each phase revealed 11 enhancement patterns, and seven of these showed a positive predictive value of nearly 100% for the pathological diagnosis (Table 1). For nodules with hyper-enhancement in the pure arterial phase, the hyper-hyper-hyper pattern was estimated to be benign. Meanwhile, the hyper-iso-hypo and hyper-hypo-hypo patterns were estimated to be Md. Nodules showing the iso-iso-hypo pattern were estimated to be Wd. For nodules with hypo-enhancement in the pure arterial phase, the hypo-iso-iso and the hypo-hypo-hypo pattern were estimated to be Wd. Another pattern, hypo-hyper-hypo, was considered to indicate Pd. The remaining four patterns corresponded to two (benign ≥ Wd, or Pd > Wd) or four pathological diagnoses. The hyper-hyper-hypo pattern, which was the most common, was seen at all histological grades as well as in benign nodules.

The covariance-adjusted sensitivity gave the exact posterior probability, and the sum of the positive predictive values for the four different diagnoses was 1 (100%). When different prior probalilities were used, some combinations of patterns resulted in a change of the most probable diagnosis (data not shown).

Findings in the early portal phase according to the HCC differentiation

In Wd HCC (early HCC), there were seven enhancement patterns, thought to be characterized by various hemodynamic changes, as compared to only three patterns for Md or Pd. Among the three patterns allowing a diagnosis of Wd HCC, two were hypo in the pure arterial phase. Subsequent iso-enhancement in the early portal phase indicated a portal flow supply which was recognizable with inflow-time mapping (Figure 1). Another early HCC, showing hyper-enhancement, is displayed in Figure 2.

In Md HCC, all three patterns were hyper in the pure arterial and hypo in the subsequent phase. If a nodule was hyper or iso/hypo in the early portal phase, the respective likelihoods of being Md HCC were 38% and 100%. Thus, decreased enhancement in the early portal phase allows a diagnosis of Md HCC (Figure 3).

Of the three patterns observed in Pd HCC, two showed the hypo finding in both the pure arterial and the subsequent phase. If the hypo-enhancement changed to hyper or iso in the early portal phase, the probabilities of these two patterns with a diagnosis of Pd HCC were 100% and 65%, respectively. More specifically, a diagnosis of Pd HCC was possible based on gradual enhancement observed from the pure arterial to the early portal phase. This finding, which depended on arterial flow, was confirmed by the time-intensity curve (Figure 4).

All benign nodules, with the exception of three large regenerative nodules, showed hyper-enhancement in both the pure arterial and the early portal phase,

Table 1. Enhancement patterns for pathological diagnosis of HCC

Nodule enhancement pattern				Pathological diagnosis			
Pure arterial phase	Early portal phase	Subsequent phase	(*n*)	Poorly differentiated (*n* = 8)	Moderately differentiated (*n* = 73)	Well-differentiated (*n* = 37)	Benign nodule (*n* = 28)
Hyper	Hyper	Hyper	9				9 (100%*)
Hyper	Hyper	Iso	14			4 (23.2%)	10 (76.8%)
Hyper	Hyper	Hypo	46	4 (40.5%)	34 (37.7%)	2 (4.4%)	6 (17.4%)
Hyper	Iso	Hypo	16		16 (100%)		
Hyper	Hypo	Hypo	23		23 (100%)		
Iso	Iso	Iso	7			4 (50.2%)	3 (49.8%)
Iso	Iso	Hypo	2			2 (100%)	
Hypo	Hyper	Hypo	2	2 (100%)			
Hypo	Iso	Hypo	7	2 (64.9%)		5 (35.1%)	
Hypo	Iso	Iso	14			14 (100%)	
Hypo	Hypo	Hypo	6			6 (100%)	

*The positive predictive values are in parentheses.

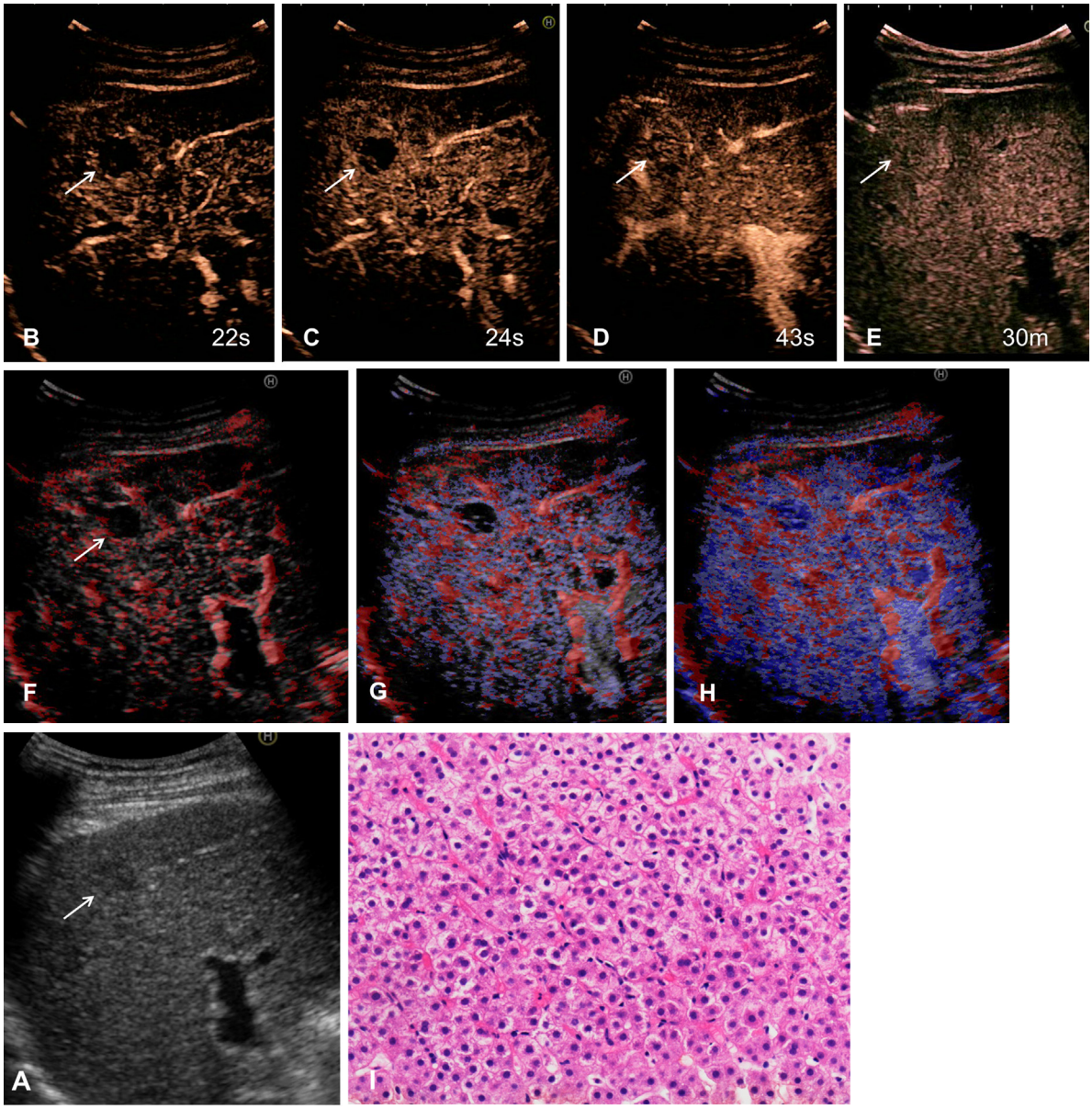

Figure 1. Hypovascular well-differentiated HCC findings on Sonazoid CEUS. A hypoechoic 1.2-cm tumor with an unclear margin on B-mode US **(A)**. In the pure arterial phase, the tumor remains hypo **(B)**, followed by hypo to iso enhancement in the early portal phase **(C, D)**. Iso-enhancement persists at 30 min **(E)**. Inflow time-mapping (ITM) shows red pixels in the artery and liver parenchyma, while there is no arterial flow inside the tumor **(F)**. After the portal flow is detected, the tumor vessels and tumor are enhanced appearing blue **(G, H)**. The biopsy specimen showed well-differentiated HCC **(I)**.

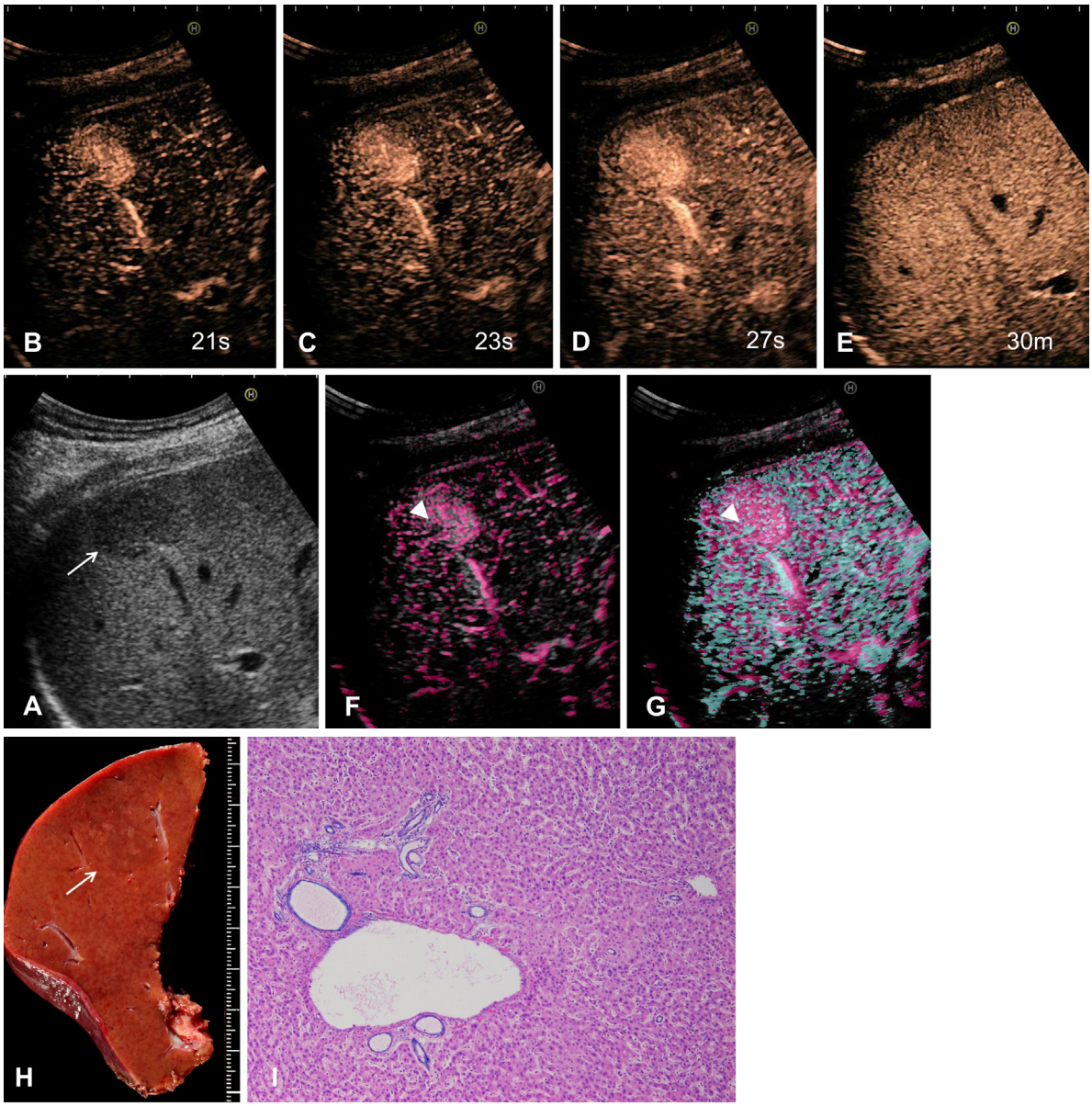

Figure 2. Hypervascular well-differentiated HCC findings on Sonazoid CEUS. A 1.7-cm hypoechoic nodule with ill-defined margins on B-mode US **(A)** shows hyper-enhancement in the pure arterial phase **(B)** and continued peripheral enhancement in the early portal phase **(C, D)**. Mild hypo-enhancement changes at 30 minutes **(E)**. On ITM, central enhancement is pink in the pure arterial phase **(F)**, and a mixed green periphery is clearly demonstrated in the early portal phase **(G)**. Residual portal vein (arrow head) is noted inside the tumor. Early HCC was confirmed by histopathological examination of the resected specimen **(H, I)**.

i.e., no remarkable change in the early portal phase. Hyper-enhancement in all three phases leads to a definitive diagnosis of benign nodules. However, hypo-enhancement change in the subsequent phase requiring differentiation from HCC was observed in all HCA, FNH, and alcoholic hyperplastic nodules.

Discussion

Imaging phases during CEUS can be divided into the vascular phase including the arterial, portal or portal venous and late phases, and the post-vascular phase (*5,14*). Changes in nodule enhancement after injection of contrast agent, observed based on these phases, are applicable to the diagnosis of liver tumors, although the optimal times are actually variable. The arterial phase is observed up to 30 seconds, 45-50 seconds or within one minute (*5*) after injection of a contrast agent, followed by the portal or portal venous phase observations made mainly after one minute. However, considering the multi-step carcinogenesis process of HCC development, ascertaining early hemodynamic changes is important. Particularly for the diagnosis of early HCC, an accurate determination of portal flow involvement is essential. Kudo *et al*. confirmed the pure arterial phase using the time-intensity curve and examined arterial and portal supplies in cases with early HCC, reporting the importance of pure arterial imaging (*15*). In this study, we divided the arterial phase (up to 45 seconds) into the pure arterial and the early portal phase and identified

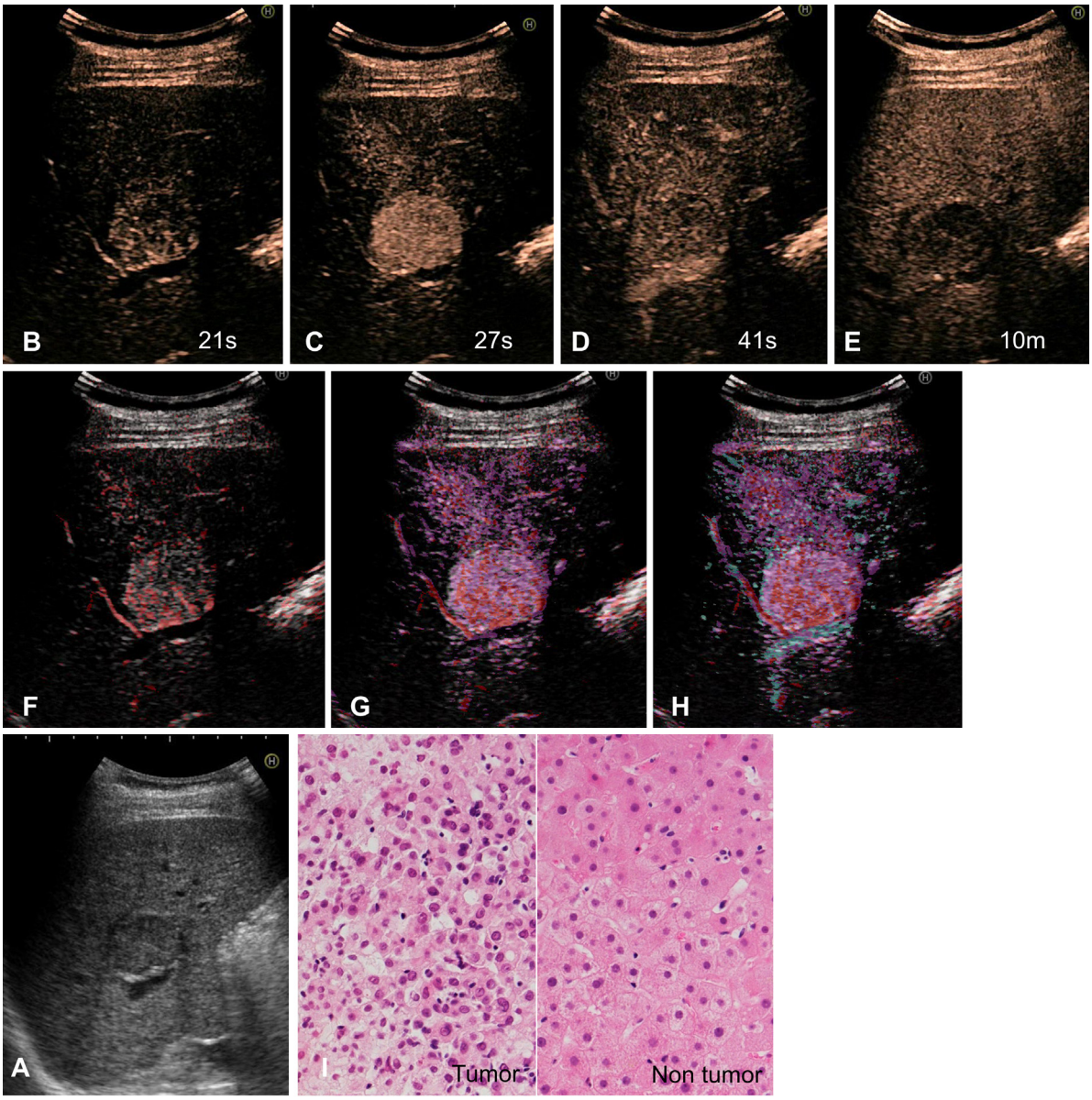

Figure 3. Moderately differentiated HCC findings on Sonazoid CEUS. A 2.5-cm hypoechoic nodule on B-mode US **(A)** showed hyper-enhancement in the pure arterial phase **(B, C)**, slight hypo-enhancement changes in the early portal phase **(D)**, and subsequent hypo-enhancement **(E)** on CEUS. On ITM, the feeding artery and nodule both appear red, then the periphery violet as time elapses in the pure arterial phase **(F, G)**. The portal flow appears green, and the parenchyma maps as a mixture of red and green in the early portal phase. There is no portal flow to this tumor because it never appears green **(H)**. The biopsy specimen confirmed the diagnosis of Md HCC **(I)**.

early hemodynamic changes in these two phases with the aim of diagnosing the histological grade of HCC.

HCC differentiation is determined in the arterial phase based on morphology and the degree of enhancement (*6,16,17*), as well as the timing of washout in the portal venous phase or the post-vascular phase (*18,19*). In particular, Sonazoid is taken up by the Kupffer cells of the liver, thereby producing stable images in the post-vascular phase. Several reports describing the advantages of CEUS for determining the degree of HCC differentiation focused on the post-vascular phase (*20,21*). Although the reported results vary somewhat depending on the imaging phase observed, most are relatively consistent. Wd or early HCC is hypo-iso vascular, while Md and Pd are hyper-vascular, although Pd shows earlier washout than Md HCC (*22*). Wang *et al*. found early HCC to show iso-enhancement in the post-vascular phase, allowing it to be differentiated from Pd or Md in post-vascular phase images. They stated that more attention should be paid to findings in the portal and the post-vascular phases rather than those in the arterial phase (*23*).

However, early stage HCC, unlike other tumors, is characteristically affected by the dual blood supply. Matsui *et al*. demonstrated these sequential blood flow changes in early stage HCC by CT (*24*). We defined the early portal phase to determine whether a diagnosis of early HCC is possible by focusing on the pure arterial

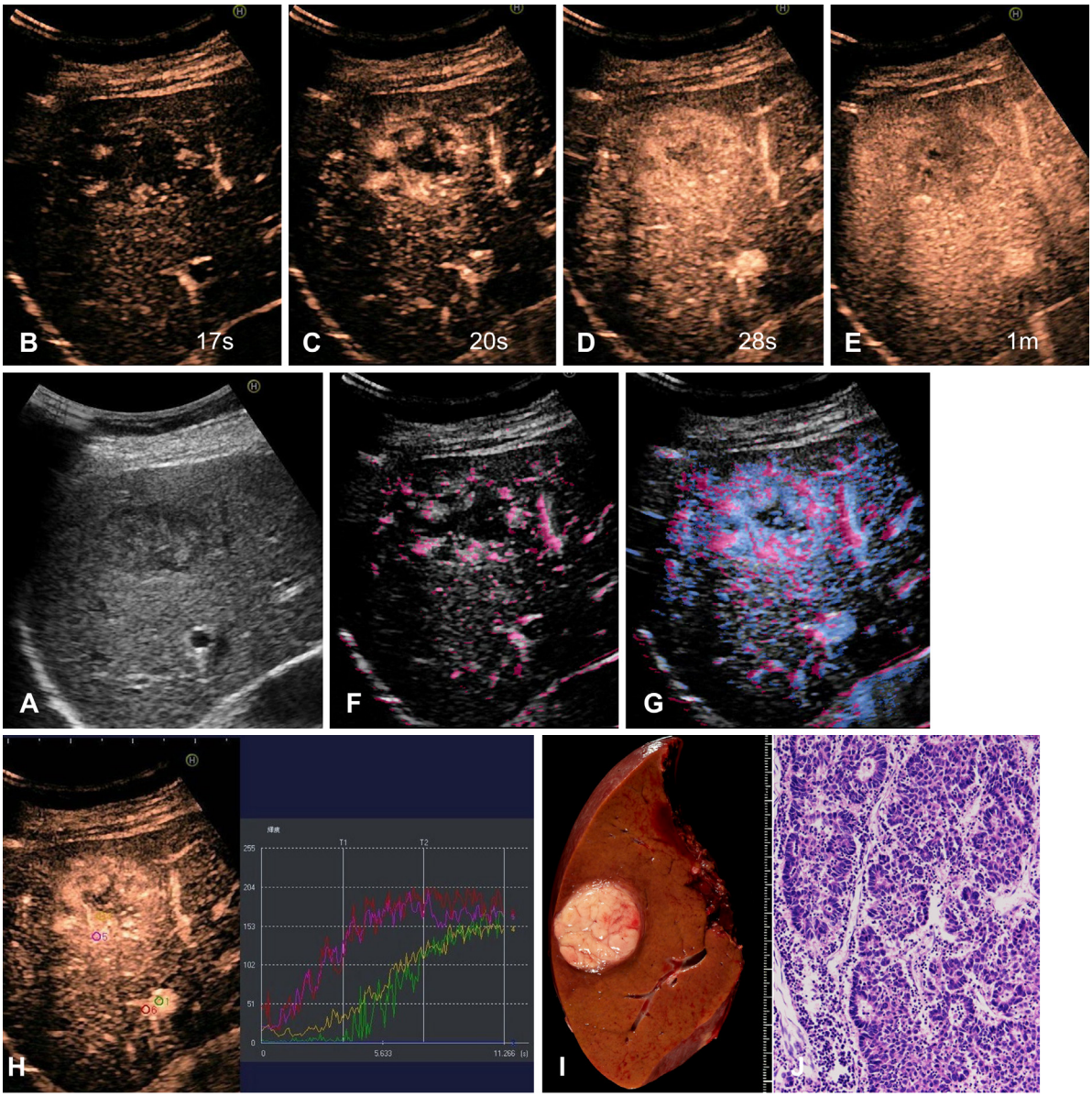

Figure 4. Poorly differentiated HCC findings on Sonazoid CEUS. A 3-cm tumor has an irregular shape and uneven internal echo on B-mode **(A)**. Gradual enhancement is seen during the pure arterial **(B)** and early portal phases **(C, D)**, followed by hypo-enhancement change at 1 minute. **(E)**. ITM shows red pixels in the tumor periphery initially **(F)**, with blue gradually appearing inside the tumor during the early portal phase **(G)**. These color changes are entirely due to arterial flow. The intensity curve for the internal portion of the nodule (yellow line) is similar to that of the periphery (violet line) **(H)**. The diagnosis of Pd HCC was confirmed by hepatic resection **(I, J)**.

and early portal phase hemodynamics. We identified various hemodynamic changes, corresponding to seven distinct enhancement patterns, in cases with early HCC. These patterns may have reflected blood supply changes from early to advanced HCC, *i.e.*, the portal vein disappears due to portal tract invasion (stromal invasion) (*11*) followed by gradual arterial proliferation. In addition, in all but one of the patterns, enhancement changes were slight (hypo- to iso- or iso- to hyper-enhancement). The same tendency was reported based on enhancement patterns of three phases (arterial, portal/portal venous, and post vascular phases) on CEUS (*8*). Our study focused only on the early phase hemodynamics and the subsequent phase, *i.e.* that after one minute which includes all except the arterial phase, to simplify the results. Finally, we obtained three patterns achieving a positive predictive value of 100% for the diagnosis of Wd HCC (early HCC).

Meanwhile, even in Md or Pd HCC supplied mainly by arterial flow, enhancement changes occurred in the early portal phase. For more than half of Md nodules, decreased enhancement was found in the early portal phase, whereas half of Pd nodules showed gradual enhancement from the pure arterial phase to the early portal phase. Early washout (within one minute) is reportedly observed in 5% of HCC (*2*). Detailed information on early hemodynamics as visualized by CEUS is thus provided by this study.

In summary, Sonazoid-enhanced ultrasound was performed to determine enhancement changes in the pure arterial, early portal, and subsequent phases for determination of the degree of HCC differentiation. A positive predictive value of 100% was obtained for the following seven patterns: three (iso-iso-hypo, hypo-iso-iso, and hypo-hypo-hypo) for Wd, two (hyper-iso-hypo and hyper-hypo-hypo) for Md, one (hypo-hyper-hypo) for Pd, and one (hyper-hyper-hyper) for benign nodules. Even in the early portal phase, hemodynamic changes were visible not only in Wd HCC but also in the Md and Pd HCC.

The major limitation of this study was small sample size because of the limited number of resection and biopsy cases, which may have given rise to bias.

Conclusion

With division of the early hemodynamics of CEUS into pure arterial and early portal phases, this modality can provide information useful for determining the likely degree of HCC differentiation and for distinguishing early stage HCC from benign nodules, and for considering the subsequent biopsy and treatment strategies.

Acknowledgements

We express our sincere appreciation to Professor Toshio Fukusato at Teikyo University for investigation of the pathological findings and Dr. Bierta Barfod for English proofreading.

Ethics statement

All procedures followed were in accordance with the ethical standards of the responsible committee on human experimentation and with the Helsinki Declaration of 1975, as revised in 2008. Informed consent was obtained from all patients for inclusion in this study.

Funding: None.

Conflict of Interest: The authors have no conflict of interest to disclose.

References

1. Bruix J, Sherman M; American Association for the Study of Liver Diseases. Management of hepatocellular carcinoma: an update. Hepatology. 2011; 53:1020-1022.
2. Terzi E, Iavarone M, Pompili M, Veronese L, Cabibbo G, Fraquelli M, Riccardi L, De Bonis L, Sangiovanni A, Leoni S, Zocco MA, Rossi S, Alessi N, Wilson SR, Piscaglia F; CEUS LI-RADS Italy study group collaborators: Contrast ultrasound LI-RADS LR-5 identifies hepatocellular carcinoma in cirrhosis in a multicenter restropective study of 1,006 nodules. J Hepatol. 2018; 68:485-492
3. Kokudo N, Takemura N, Hasegawa K, *et al*. Clinical practice guidelines for hepatocellular carcinoma: The Japan Society of Hepatology 2017 (4th JSH-HCC guidelines) 2019 update. Hepatol Res. 2019; 49:1109-1113.
4. Yanagisawa K, Moriyasu F, Miyahara T, Yuki M, Iijima H. Phagocytosis of ultrasound contrast agent microbubbles by Kupffer cells. Ultrasound Med Biol. 2007; 33:318-325.
5. Lee JY, Minami Y, Choi BI, *et al*. The AFSUMB Consensus Statements and Recommendations for the Clinical Practice of Contrast-Enhanced Ultrasound using Sonazoid. Ultrasonography. 2020; 39:191-220.
6. Hayashi H, Nishigaki Y, Tomita E, Watanabe C, Watanabe S, Watanabe N, Suzuki Y, Kato T, Naiki T. Usefulness of early vascular phase images from contrast-enhanced ultrasonography using Sonazoid for the diagnosis of hypovascular hepatocellular carcinoma. Hepatol Res. 2016; 46:497-504.
7. Kita R, Sakamoto A, Nagata Y, Nishijima N, Ikeda A, Matsuo H, Okada M, Ashida S, Taniguchi T, Kimura T, Osaki Y. Visualization of blood drainage area from hypervascular hepatocellular carcinoma on ultrasonographic images during hepatic arteriogram: Comparison with depiction of drainage area on contrast-enhanced ultrasound. Hepatol Res. 2012; 42:999-1007.
8. Numata K, Fukuda H, Miwa H, Ishii T, Moriya S, Kondo M, Nozaki A, Morimoto M, Okada M, Takebayashi S, Maeda S, Nozawa A, Nakano M, Tanaka K. Contrast-enhanced ultrasonography findings using a perflubutane-based contrast agent in patients with early hepatocellular carcinoma. Eur J Radiol. 2014; 83:95-102.
9. Yoshikawa H, Azuma T, Kawabata K, Sasaki K, Umemura S. Inflow-Time Mapping of Microbubbles Based on Ultrasonic Contrast Images for Differential Tumor Diagnosis. IEEE International Ultrasonic Symposium 2008, China; Abstract Book: 369-370.
10. International Consensus Group for Hepatocellular Neoplasia. Pathologic diagnosis of early hepatocellular carcinoma: a report of the international consensus group for hepatocellular neoplasia. Hepatology. 2009; 49:658-664.
11. Nakano M, Saito A, Yamamoto M, Doi M, Takasaki K. Stromal and blood vessel wall invasion in well-differentiated hepatocellular carcinoma. Liver. 1997; 17:41-46.
12. Fukusato T, Soejima Y, Kondo F, Inoue M, Watanabe M, Takahashi Y, Aso T, Uozaki H, Sano K, Sanada Y, Niki T. Preserved or enhanced OATP1B3 expression in hepatocellular adenoma subtypes with nuclear accumulation of β-catenin. Hepatol Res. 2015; 45:E32-42.
13. Jones G, Johnson WO, Hanson TE, Christensen R. Identifiability of models for multiple diagnostic testing in the absence of a gold standard. Biometrics. 2010; 66:855-863.
14. Dietrich CF, Nolsøe CP, Barr RG, *et al*. Guidelines and Good Clinical Practice Recommendations for Contrast-Enhanced Ultrasound (CEUS) in the Liver-Update 2020 WFUMB in Cooperation with EFSUMB, AFSUMB, AIUM, and FLAUS. Ultrasound Med Biol. 2020; 46:2579-2604.
15. Kudo M, Hatanaka K, Inoue T, Maekawa K. Depiction of portal supply in early hepatocellular carcinoma and dysplastic nodule: value of pure arterial ultrasound

imaging in hepatocellular carcinoma. Oncology. 2010; 78 Suppl 1:60-67.
16. Sugimoto K, Shiraishi J, Moriyasu F, Doi K. Computer-aided diagnosis for contrast-enhanced ultrasound in the liver. World J Radiol. 2010; 2:215-223.
17. Tanaka H, Iijima H, Higashiura A, *et al*. New malignant grading system for hepatocellular carcinoma using the Sonazoid contrast agent for ultrasonography. J Gastroenterol. 2014; 49:755-763.
18. Takahashi M, Maruyama H, Ishibashi H, Yoshikawa M, Yokosuka O. Contrast-enhanced ultrasound with perflubutane microbubble agent: evaluation of differentiation of hepatocellular carcinoma. AJR Am J Roentgenol. 2011; 196:W123-131.
19. Murata K, Saito A, Katagiri S, Ariizumi S, Nakano M, Yamamoto M. Association of des-γ-carboxy prothrombin production and Sonazoid-enhanced ultrasound findings in hepatocellular carcinomas of different histologic grades. J Med Ultrason. 2018; 45:223-229.
20. Arita J, Hasegawa K, Takahashi M, Hata S, Shindoh J, Sugawara Y, Kokudo N. Correlation between contrast-enhanced intraoperative ultrasound using Sonazoid and histologic grade of resected hepatocellular carcinoma. AJR Am J Roentgenol. 2011; 196:1314-1321.
21. Tada T, Kumada T, Toyoda H, Ito T, Sone Y, Kaneoka Y, Maeda A, Okuda S, Otobe K, Takahashi K. Utility of Contrast-enhanced Ultrasonography with Perflubutane for Determining Histologic Grade in Hepatocellular Carcinoma. Ultrasound Med Biol. 2015; 41:3070-3078.
22. Jang HJ, Kim TK, Burns PN, Wilson SR. Enhancement patterns of hepatocellular carcinoma at contrast-enhanced US: comparison with histologic differentiation. Radiology. 2007; 244:898-906.
23. Wang F, Numata K, Nakano M, Tanabe M, Chuma M, Nihonmatsu H, Nozaki A, Ogushi K, Luo W, Ruan L, Okada M, Otani M, Inayama Y, Maeda S. Diagnostic Value of Imaging Methods in the Histological Four Grading of Hepatocellular Carcinoma. Diagnostics (Basel). 2020; 10:321.
24. Matsui O, Kobayashi S, Sanada J, Kouda W, Ryu Y, Kozaka K, Kitao A, Nakamura K, Gabata T. Hepatocelluar nodules in liver cirrhosis: hemodynamic evaluation (angiography-assisted CT) with special reference to multi-step hepatocarcinogenesis. Abdom Imaging. 2011; 36:264-272.

Received September 25, 2020; Revised October 22, 2020; Accepted October 26, 2020.

Released online in J-STAGE as advance publication October 28, 2020.

**Address correspondence to*:
Akiko Saito, Gastroenterology and Hepatology, National Center for Global Health and Medicine, 1-21-1 Toyama, Shinjuku-ku, Tokyo162-8655, Japan.
E-mail: akisaito@hosp.ncgm.go.jp